10–100 keV ELECTRON ACCELERATION AND EMISSION FROM SOLAR FLARES

R. P. LIN

Space Sciences Laboratory, University of California, Berkeley, Calif. 94720, U.S.A.

and

H. S. HUDSON*

Department of Physics, University of California, San Diego, La Jolla, Calif. 92038, U.S.A.

(Received 17 November, 1970)

Abstract. We present an analysis of spacecraft observations of non-thermal X-rays and escaping electrons for 5 selected small solar flares in 1967. OSO-3 multi-channel energetic X-ray measurements during the non-thermal component of the solar flare X-ray bursts are used to derive the parent electron spectrum and emission measure. IMP-4 and Explorer-35 observations of >22 keV and >45 keV electrons in the interplanetary medium after the flares provide a measure of the total number and spectrum of the escaping particles. The ratio of electron energy loss due to collisions with the ambient solar flare gas to the energy loss due to bremsstrahlung is derived. The total energy loss due to collisions is then computed from the integrated bremsstrahlung energy loss during the non-thermal X-ray burst. For >22 keV flare electrons the total energy loss due to collisions is found to be $\sim 10^4$ times greater than the bremsstrahlung energy loss and $\sim 10^2$ times greater than the energy loss due to escaping electrons. Therefore the escape of electrons into the interplanetary medium is a negligible energetic electron loss mechanism and cannot be a substantial factor in the observed decay of the non-thermal X-ray burst for these solar flares.

We present a picture of electron acceleration, energy loss and escape consistent with previous observations of an inverse relationship between rise and decay times of the non-thermal X-ray burst and X-ray energy. In this picture the acceleration of electrons occurs throughout the 10–100 sec duration of the non-thermal X-ray burst and determines the time profile of the burst. The average energy of the accelerated electrons first rises and then falls through the burst. Collisions with the ambient gas provide the dominant energetic electron loss mechanism with a loss time of $\lesssim 1$ sec. This picture is consistent with the ratio of the total number of energetic electrons accelerated in the flare to the maximum instantaneous number of electrons in the flare region. Typical values for the parameters derived from the X-ray and electron observations are:

total energy in >22 keV electrons $\approx$ total energy lost by collisions $= \sim 10^{28-29}$ erg,
total number of electrons accelerated above 22 keV $= \sim 10^{36}$,
total energy lost by non-thermal bremsstrahlung $= \sim 10^{24}$ erg,
total energy lost in escaping >22 keV electrons $= \sim 10^{26}$ erg,
total number of >22 keV electrons escaping $= \sim 10^{33-34}$.

The total energy in electrons accelerated above 22 keV is comparable to the energy in the optical or quasi-thermal flare, implying a flare mechanism with particle acceleration as one of the dominant modes of energy dissipation.

The overall efficiency for electron escape into the interplanetary medium is ~ 0.1–1% for these flares, and the spectrum of escaping electrons is found to be substantially harder than the X-ray producing electrons.

1. Introduction

The acceleration of particles to non-thermal energies is a phenomenon which is

* Currently at Tokyo Astronomical Observatory, Mitaka, Tokyo, Japan.

Solar Physics **17** (1971) 412–435.

prevalent in the tenuous plasmas found throughout the universe. Examples in our own solar system of particle acceleration in plasmas include the terrestrial magnetosphere and magnetotail, the Jovian magnetosphere, interplanetary shock waves and solar flares. Particle acceleration in solar flares has been found to generate both energetic ions and electrons. Extensive spacecraft observations of energetic solar particles have shown that 10–100 keV electrons are accelerated and emitted by solar flares much more frequently than energetic protons (Lin, 1970a). Energetic electrons, unlike protons, produce radio and X-ray emission in the solar atmosphere which is observable from the earth or from earth orbiting spacecraft.

X-ray observations (Hudson *et al.*, 1969) show that essentially every flare or subflare is accompanied by X-ray emission above 7.7 keV. Although most of these solar flare X-ray bursts appear to be quasi-thermal emission due to the heating of the solar flare plasma to $0.5\text{–}3 \times 10^7$ K, many of the bursts also contain a non-thermal X-ray component (Kane and Anderson, 1970). The non-thermal component is characterized by rapid time variations, with rise and decay times typically a few seconds, and power law energy spectra. In contrast the quasi-thermal component smoothly varies on a time scale of minutes and has an energy spectrum too soft to measure by present scintillation techniques (see Kane and Hudson, 1970).

On many occasions following solar flares with energetic ($\gtrsim$20 keV) X-ray bursts, electrons are observed in the interplanetary medium, particularly if the flare is located favorably for the propagation of these electrons to the vicinity of the observing spacecraft. Over 100 events with $>$40 keV electron flux above $10(\text{cm}^2 \text{ sec ster})^{-1}$ have been observed in the ascending portion (1964–67) of this solar cycle. Moreover, the limited angular cone of propagation ($\sim 30°$) of these electron events imply that over 10^3 events above that threshold have been emitted by the Sun during this period. Many examples of such events have been published previously, including three of the events to be discussed here (see Lin, 1970b).

Previous studies of energetic electrons in solar flares (see for example Anderson and Winckler, 1962; Takakura, 1969; Arnoldy *et al.*, 1968; Holt and Cline, 1968; and Kane and Anderson, 1970) have concentrated on the interpretation of the observed solar radio and X-ray emission. In this paper we analyze the behavior of the 10–100 keV electron component produced in solar flares by examining the non-thermal X-ray burst and the fluxes of electrons escaping into the interplanetary medium. X-ray and electron observations for five solar flare events occurring during the period of data overlap between the OSO-3 energetic X-ray experiment and the electron experiments aboard IMP-4 and Explorer-35 are presented. From these observations we infer parameters and conditions of 10–100 keV electron acceleration and emission by solar flares. Our analysis of the dynamical processes affecting energetic electrons in the solar atmosphere proceeds as follows:

(1) Using the non-thermal component of the X-ray burst, we derive the parent electron energy spectrum and the 'emission measure' $n_e n_i V$, at time of maximum (n_e = non-thermal electron density, n_i = ambient ion density, V = volume).

(2) The electron observations at $\sim$1 AU in the interplanetary medium are extra-

polated back to obtain the energy spectrum and total number of electrons escaping from the Sun.

(3) We calculate the ratio of collision to bremsstrahlung loss for an electron of a given energy. From the total integrated bremsstrahlung energy loss observed during an X-ray burst the total energy loss due to electron collisions with the ambient medium is obtained.

(4) The total energy contained in escaping electrons is compared to the energy lost by collision to determine the relative importance of these two processes in the decay of the X-ray burst. We examine the energy dependence of the escape mechanism by comparing the energy spectra of the X-ray producing electrons and the escaping electrons.

(5) Estimates are made of the height of the acceleration region and the time scale of the acceleration process, based on the picture of the solar flare electron phenomenon derived in parts 1–4.

(6) The total energy contained in the $\gtrsim 22$ keV electrons is compared to the quasi-thermal flare energy and the implications are discussed.

2. Observations

A. ELECTRON OBSERVATIONS

The observations of electrons in the interplanetary medium are from the University of California (Berkeley) experiments aboard IMP-4 and Explorer 35. These experiments contained detectors sensitive to >22 keV and >45 keV electrons, and >0.3 MeV protons. Electrons are unambiguously identified by the instrumentation. Lin (1970a) gives a full description of the instrumentation.

Only impulsive electron events will be considered here. These events have relatively simple time profiles and can be identified with specific solar flares. Their fast rise-slow decay time profiles suggest a short injection time followed by a longer period of diffusion, or storage and release. Fifty-seven prompt electron events occurred during the interval of the present study, 9 March 1967 to 31 March 1968; improved instrumentation available after 24 May 1967 detected an additional 25 weak prompt solar electron events. No satellite data exists for the period 8–24 May 1967. For each event in the list, an Hα flare was selected as the most likely source for the particle injection. The selection process included reference to the solar radio emission occurring at the time of the flare. The resulting list of flares conforms to the characteristics ascribed to electron-associated flares by Lin and Anderson (1967); their longitudes generally fall in the western hemisphere and they frequently have small optical importance classifications.

B. X-RAY OBSERVATIONS

The OSO-3 hard X-ray telescope provided the comparison X-ray data. This instrument (Hudson *et al.*, 1969) responds to X-rays above 7.7 keV energy and has six logarithmically-spaced differential energy channels ranging up to 210 keV. OSO-3

gives about 55 per cent data coverage, and many thousands of X-ray bursts occurred during the interval of this study. Solar X-ray bursts correlate very well with Hα flares, so that a well-identified X-ray burst corresponded to each member of the list of solar flares associated with electron emission.

In many solar X-ray bursts both components, impulsive and slow, can be observed. The slow, quasi-thermal component has a very steep energy spectrum, presumably of the form

$$\frac{\mathrm{d}J(h\nu)}{\mathrm{d}(h\nu)} \propto A \frac{n_e n_i V}{h\nu\sqrt{kT}} e^{-(h\nu/kT)} \quad \text{photons (cm}^2 \text{ sec keV)}^{-1} \tag{1}$$

where $h\nu$ is the photon energy. The temperature T falls in the range $0.5\text{–}3 \times 10^7$ K and the emission measure $n_e n_i V$ takes values between 10^{47} and 10^{50} cm^{-3}. The quasi-

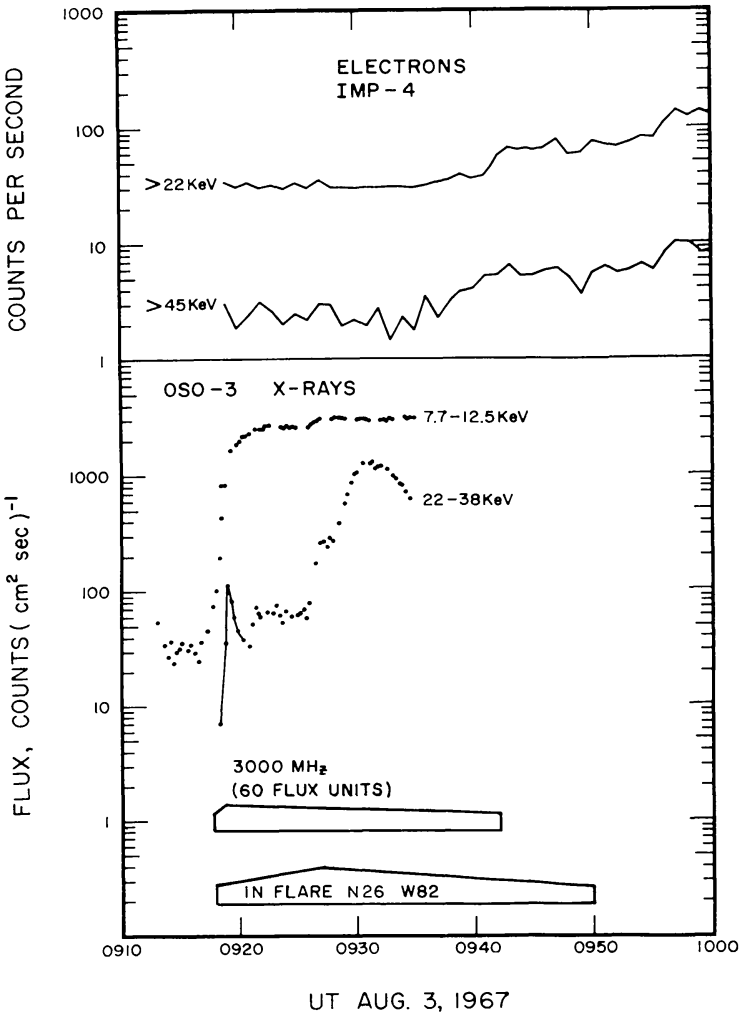

Fig. 1. X-ray and electron observations for the event of 3 August 1967 are presented here along with the optical and 3000 MHz radio emission. The X-ray channels are chosen to show the quasi-thermal component (7.7–12.5 keV) and the non-thermal component (dots connected by lines in the 22–38 keV channel). The 7.7–12.5 keV counting rate reached saturation, ~ 3000 cm^{-2} sec^{-1} and the 22–38 keV channel is recording pile-up counts after the non-thermal burst (see Kane and Hudson, 1970). The electron onset at 1 AU is observed at about 09^h35^m UT in the > 45 keV channel.

thermal component usually dominates the counting rate of the 7.7–12.5 keV channel. The spectrum of the non-thermal component can be represented by a power law with exponent φ,

$$\frac{dJ(h\nu)}{d(h\nu)} \propto B(h\nu)^{-\varphi} \quad \text{photons} \quad (\text{cm}^2\ \text{sec keV})^{-1} \tag{2}$$

in the energy range 10–100 keV (Kane and Anderson, 1970). The quasi-thermal spectrum presumably arises in free–free and free–bound radiation from a Maxwellian distribution of electron velocities, while the non-thermal emission comes from the bremsstrahlung of a power law electron energy spectrum.

The non-thermal component of the spectrum has a duration of ~10–100 sec. The OSO-3 experiment samples a complete spectrum each 15.36 sec and cannot resolve some features of the impulsive non-thermal emission. The non-thermal component occurs during the onset phase of some quasi-thermal bursts, but not all solar X-ray bursts have detectable non-thermal emission.

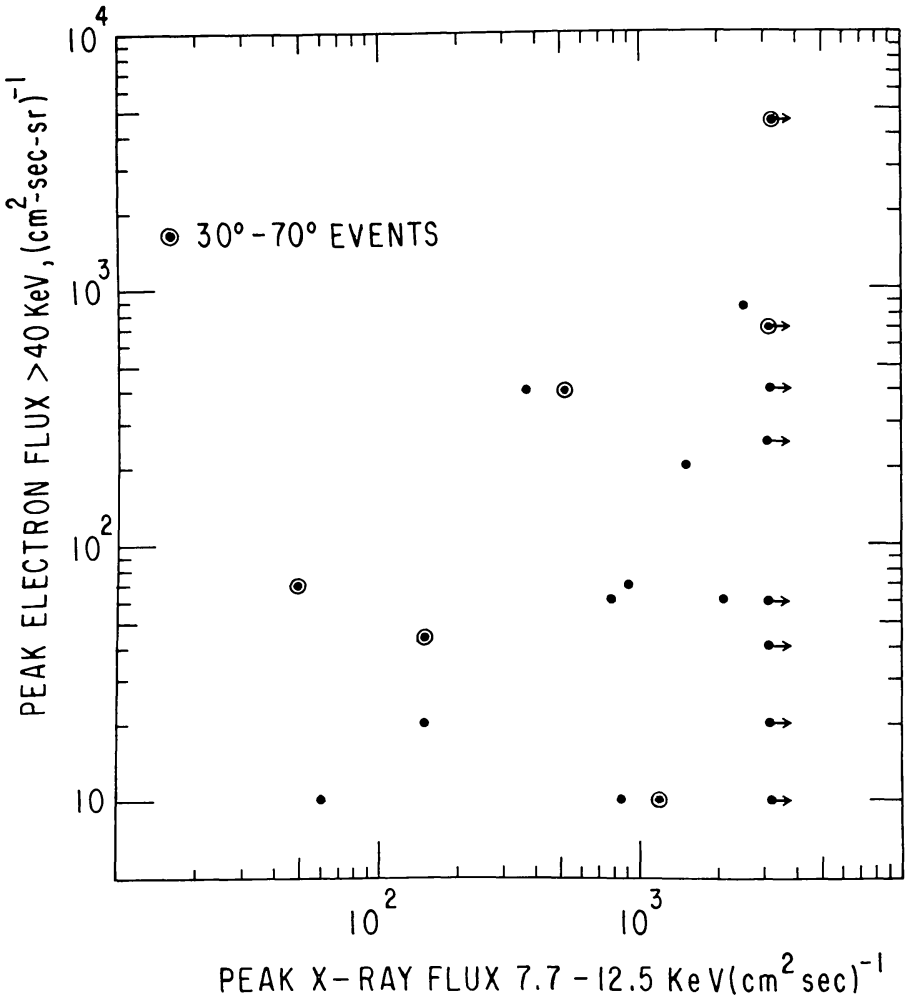

Fig. 2. The peak > 40 keV electron flux observed at 1 AU is plotted against the peak quasi-thermal 7.7–12.5 keV X-ray flux. Note that no events are observed in the upper left hand corner and that the 30°–70° solar longitude events appear to give relatively larger electron fluxes.

C. EVENT SELECTION

An examination of OSO-3 X-ray data associated with the 82 electron events occurring during the interval of study yielded 25 for which the X-ray data coverage included the probable time of the associated X-ray bursts. Of these, 24 showed well-correlated X-ray bursts. Five of these X-ray bursts produced clearly recognizable non-thermal emission while eight did not. These five non-thermal events will be analyzed here. Of the others, one burst saturated the detector and 11 did not generate a high enough counting rate for distinguishing the non-thermal and quasi-thermal components. Figure 1 shows an example of a X-ray burst displaying both components, and followed by an electron event at 1 AU.

The choice of the X-ray events for analysis is limited by the OSO-3 instrument. In intense X-ray events the non-thermal component is usually masked by pulse pileup and saturation effects due to the quasi-thermal component. Small events are not observed with sufficient counting rate in the higher channels to be analyzed. The lower limit for analysis is a >22 keV X-ray flux integrated over the burst of ~ 50 photons/cm^2. The net effect of these instrumental limitations is to choose for analysis those events containing an abnormally intense non-thermal component.

The rise and decay times of the 7.7–12.5 keV (quasi-thermal) X-ray flux during the bursts associated with electron events observed at 1 AU were compared to X-ray bursts in general, and no characteristics peculiar to the electron event associated bursts were found. However, some indications of propagation effects for the escaping electrons are evident from Figure 2, where the maximum electron flux is plotted versus the maximum X-ray flux. It appears that for the restricted longitude range, 30°–70° west, the ratio of electron flux to the X-ray flux is larger. Similar propagation effects have been reported by Arnoldy *et al.* (1968) from a comparison of ~ 20 keV X-ray bursts to electron events. The effect of the electron propagation is to favor the observation of electrons from flares near W50° solar longitude. The electron flux from events arising from flares far from this longitude appears to be attenuated or not observed at all.

3. X-Ray Burst Electrons

The flux and spectrum of the solar X-ray emission provide a measure of the number of electrons in the X-ray source and their energy spectrum if some assumptions are made about the X-ray production mechanism and region. We shall follow the procedure of Kane and Anderson (1970) in deriving the parent electron spectrum.

In view of the rapid variations of the non-thermal component and its hard energy spectrum we shall assume that isotropic bremsstrahlung produces the non-thermal component of solar X-rays. For convenience it is assumed that the production of X-rays occurs in a homogeneous region of volume V with ambient ion density n_i and energetic electron density n_e. Furthermore, we assume that the electron spectrum is of the form

$$\frac{\mathrm{d}n_e}{\mathrm{d}E} = AE^{-\delta} \tag{3}$$

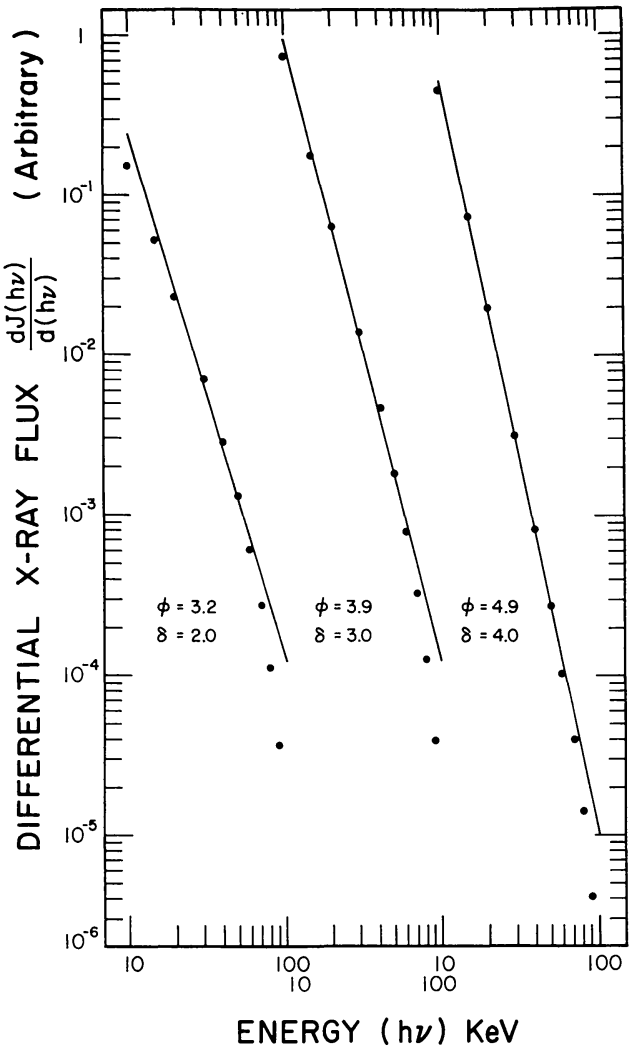

Fig. 3. The X-ray spectrum was numerically computed for electron spectra of the form $dn_e/dE = AE^{-\delta}$. For various values of δ the resulting X-ray spectrum was fitted to a power law $dJ(h\nu)/d(h\nu) = B(h\nu)^{-\varphi}$ in the energy range 20–70 keV as shown.

where n_e = number of electrons per cm^3, E = electron kinetic energy, A, δ constants; and that the spectrum falls off rapidly above 100 keV. This assumption of an energy cutoff is based on (1) the results of Kane and Anderson (1970) in which the observed spectrum of the non-thermal X-ray component agrees well with that calculated for a power law parent electron spectrum extending only to 100 keV, and (2) the escaping electron spectra observed at 1 AU for pure electron events which show a rapid fall off near 100 keV (Lin, 1970a; Lin and Anderson, 1970).

Since we are dealing with non-relativistic energy electrons we can use the Bethe-Heitler approximation for the bremsstrahlung cross-section (Jackson, 1962) written here as

$$\frac{d\sigma(h\nu, E)}{d(h\nu)} = 3.16 \times 10^{-24} \frac{1}{h\nu E} \ln\left[\left(\frac{E}{h\nu}\right)^{1/2} + \left(\frac{E}{h\nu} - 1\right)^{1/2}\right] \text{ cm}^2 \text{ ion}^{-1} \text{ keV}^{-1} \quad (4)$$

where E and $h\nu$ are in keV.

Then the differential X-ray flux observed at 1 AU is given by

$$\frac{dJ(h\nu)}{d(h\nu)} = \frac{1}{4\pi r^2} \int_{h\nu}^{100} \frac{d\sigma(h\nu, E)}{d(h\nu)} n_i V v \frac{dn_e}{dE} dE \approx 1.05 \times 10^{-42} n_i V \times$$

$$\times \left\{ \frac{1}{h\nu} \int_{h\nu}^{100} \frac{1}{E^{1/2}} \frac{dn_e}{dE} \ln \left[\left(\frac{E}{h\nu} \right)^{1/2} + \left(\frac{E}{h\nu} - 1 \right)^{1/2} \right] dE \right\}$$

$$\text{cm}^{-2}\ \text{sec}^{-1}\ \text{keV}^{-1} \qquad (5)$$

where $r = 1\ \text{AU} = 1.5 \times 10^{13}$ cm and v = electron velocity.

For electron spectra of the Form (3), $dJ(h\nu)/d(h\nu)$ for various values of δ have been numerically computed. The resultant spectra are power law over the 20–70 keV energy and fall off above 70 keV. This behavior is just that observed in the X-ray observations in small flares (Kane and Anderson, 1970). Several examples are plotted in Figure 3. We have fitted the computed X-ray spectra to a power law with exponent φ as in Equation (2) over the 20 to 70 keV range, and plotted the variation of φ with δ in Figure 4.

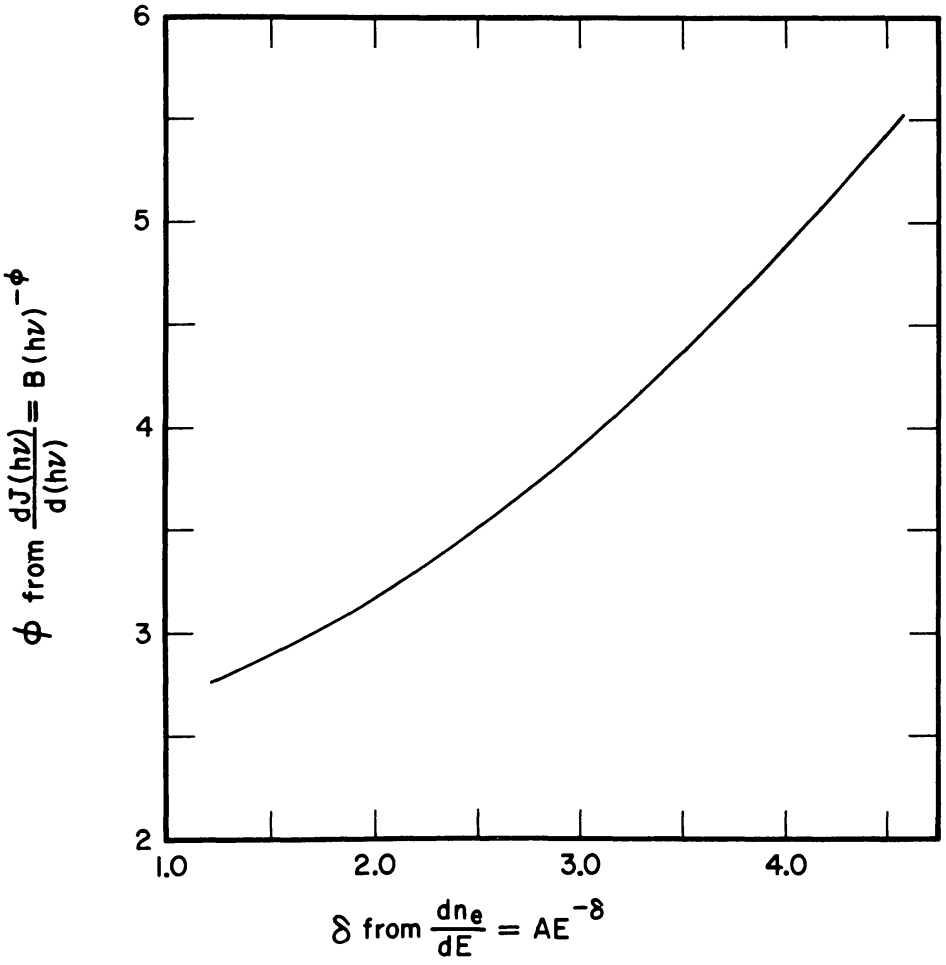

Fig. 4. From numerical calculations and fits shown in Figure 3 the variation of the X-ray spectral exponent with the electron spectral exponent was derived and plotted here. The electron spectrum is assumed to extend only to 100 keV and the X-ray spectra are fitted over the 20–70 keV range.

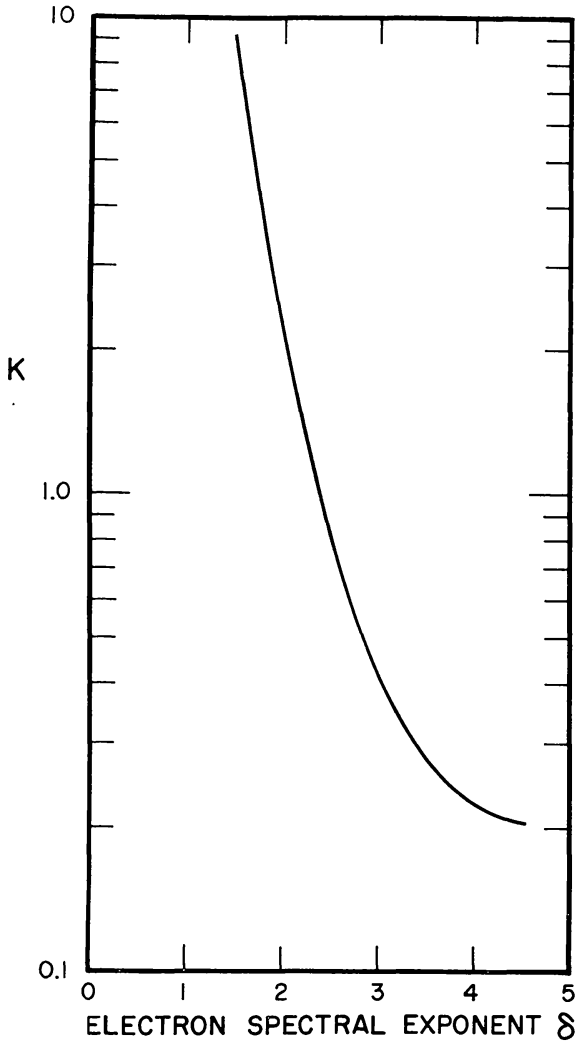

Fig. 5. The constant K which relates the emission measure to the observed photon flux as a function of the electron spectral exponent is shown here.

$$n_e(E>22\text{ keV})\,n_iV=\frac{J(22\text{ keV}<h\nu<38\text{ keV})}{6.55\times10^{-43}\,K}\left(\frac{22^{-\delta+1}-100^{-\delta+1}}{\delta-1}\right)\times$$
$$\times\left(\frac{\varphi-1}{22^{-\varphi+1}-38^{-\varphi+1}}\right)$$

Let K be the constant such that $K(h\nu)^{-\varphi}=\{\ \}$ of Equation (5). Then, the 'emission measure' n_en_iV may be derived from the X-ray observations. For electrons greater than 22 keV and $J\,(22\text{ keV}<h\nu<38\text{ keV})$,

$$n_e(E>22\text{ keV})\,n_iV=\frac{J(22\text{ keV}<h\nu<38\text{ keV})}{6.55\times10^{-43}\,K}\times$$
$$\times\left(\frac{22^{-\delta+1}-100^{-\delta+1}}{\delta-1}\right)\left(\frac{\varphi-1}{22^{-\varphi+1}-38^{-\varphi+1}}\right)\qquad(6)$$

K is graphed in Figure 5.

In channels 4 and 5 OSO-3 observes X-rays in the 22–38 keV and 38–65 keV energy

ranges, which correspond closely in parent electron energies to the 22 keV and 45 keV thresholds of the IMP detectors. Data from these two channels were used to derive φ and δ and $n_e(E>22\text{ keV})n_iV$ for each of the five events. These parameters are listed in Table I.

4. Electrons Escaping from the Sun

The >22 and >45 keV solar electron fluxes observed in the interplanetary medium can be translated back to the Sun to obtain the total number and spectrum of the escaping electrons for that flare event. From the flux intensity versus time profile of the particular event we estimate the amount of diffusion which the particles have undergone in their propagation from the Sun to 1 AU. In some of the events (notably the two on 30 July 1967) the electron flux undergoes a rapid (e-folding time $\sim$10–20 min) decay indicating essentially no scattering in the propagation of the electrons inside of 1 AU (see Lin, 1970c). For these events the total number of electrons emitted is just

$$N(E > E_0) = 2\pi\Omega r^2 \int_0^\infty J(E > E_0, t)\,\mathrm{d}t \tag{7}$$

where $J(E>E_0, t)$ is the average directional flux $(\text{cm}^2\text{ sec ster})^{-1}$, Ωr^2 is the cross-sectional area of the cone of propagation, Ω the solid angle, $r=1$ AU. In the other events the electron flux exhibits an intensity versus time profile which is more indicative of diffusion-dominated propagation. For these events we estimate the total number of electrons through an isotropic diffusion calculation. Following Parker (1963), the particle density $\varrho(E)\,\text{cm}^{-3}\,\text{keV}^{-1}$ is governed by the diffusion equation

$$\frac{\partial \varrho}{\partial t} = \frac{1}{r^2}\frac{\partial}{\partial r}\left(Dr^2\frac{\partial \varrho}{\partial r}\right) \tag{8}$$

where D is the diffusion coefficient, which we assume is constant, and $r=$distance from source, $t=$time. The solution to this equation is

$$\varrho = \frac{1}{\Omega}\left(\frac{\mathrm{d}N}{\mathrm{d}E}\right)\frac{\exp(-r^2/4Dt)}{2\pi^{1/2}(Dt)^{3/2}} \tag{9}$$

where Ω is the solid angle into which the particles are emitted, and $\mathrm{d}N/\mathrm{d}E$ is the escaping electron differential energy spectrum. The maximum occurs at $t=r^2/6D$, for which

$$\frac{\mathrm{d}N}{\mathrm{d}E} = 2\pi\Omega r^3\,\frac{\varrho_{\max}\exp(\frac{3}{2})}{(216\pi)^{1/2}} \tag{10}$$

Since $\varrho=4\pi/v\;\mathrm{d}J/\mathrm{d}E$, integrating over energy we obtain for the total number of escaping electrons

$$N(E > E_0) = 2\pi\Omega r^3\left[\left(\frac{2\pi}{27}\right)^{1/2} e^{3/2}\,\frac{J_{\max}(E > E_0)}{\bar{v}}\right] \tag{11}$$

where $v=$velocity of the particle, $\bar{v}$ the average velocity of particles with energy greater than E_0. Note that this expression for $N(E>E_0)$ is independent of D, depending only

TABLE I

A comparison of X-ray producing electrons and escaping electrons

Date 1967	X-ray burst maximum				Integrated X-ray burst			Escaping electrons	
	UT	$n_e(E>22$ keV$)\, n_i V$ cm^{-3}	Spectral exponent [a] φ-X-ray	δ-electron	Number of photons/cm^2 22 keV $< h\nu <$ 38 keV	Spectral exponent [a] φ-X-ray	δ-electron	Total number $E>22$ keV	Spectral exponent [a] δ
30 July	0509.4	1.15×10^{46}	4.97	4.1	4.8×10^3	5.1	4.2	2.9×10^{33}	2.97
30 July	1601.0	7.6×10^{45}	4.4	3.55	1.7×10^3	4.25	3.45	2.6×10^{33}	3.07
3 August	0921.7	2.0×10^{46}	4.7	3.85	5.8×10^3	4.8	3.95	6.7×10^{33}	3.17
25 October	2129.7	2.7×10^{45}	4.7	3.85	5.5×10^2	4.7	3.85	5.5×10^{32}	– [b]
13 December	1436.0	4.6×10^{45}	4.4 [c]	3.55 [c]	1.9×10^3	4.4	3.55	6.3×10^{32}	3.0

[a] φ from $dJ(h\nu)/d(h\nu) \sim (h\nu)^{-\varphi}$, δ from $dn_e/dE \propto E^{-\delta}$.

[b] Not sufficient flux above 45 keV to calculate spectrum.

[c] Insufficient counting rate at maximum to calculate φ and δ. These values are integrated values.

on $J_{\max}(E>E_0)$. Also note that we have neglected any attenuation due to longitude effects.

The average size of the cone of interplanetary field lines filled with electrons by an event has been estimated by Lin and Anderson (1967). Electron event flares are distributed in solar longitude with an rms deviation of 15° about a most probable longitude of ~W55°. Thus, on the average a cone of roughly 30° angular extent is filled with electrons from a single event. For a particular event this cone may be as large as 70° (see Lin, 1970b). For each of the five events studied here, the appropriate Expression, (7) or (11), and value for the size of the cone of propagation have been used to obtain the number of escaping electrons (Table I). The electron energy spectra was assumed to be power law (Equation 3) and the exponent δ was derived* and also listed in Table I.

A comparison of the two spectra, that derived from X-ray burst and that from the interplanetary electron observations, indicate that escaping electrons are more energetic. A second point of interest is that the number of electrons escaping appears small compared to the number present in the X-ray producing volume if a reasonable value of the ion density is assumed. One would expect from the observations of X-ray bursts from behind the limb of the Sun that the X-ray production region may be high in the solar chromosphere – $\gtrsim 10^4$ km above the solar photosphere – so that a reasonable value of the ion density (taking 10× Baumbach-Allen corona, from Kundu, 1965) might be $\sim 10^{10}$ cm^{-3}. If the total number of >22 keV electrons producing the X-ray burst is computed from the emission measure (Table I) it is seen to be ~3 orders of magnitude larger than the number escaping. Further comment on these comparisons are reserved for later in this paper.

5. Electron Loss by Escape and Collisions

The decay of the X-ray burst is interpreted as due to the loss of the energetic electrons from the X-ray production region. This loss can be due to either escape of the electrons from that region into a much lower density region where no observable X-ray flux is produced – the interplanetary medium or perhaps the upper corona – or loss of the electrons through collisions with the ambient gas. We estimate the relative importance of these two processes by calculating the energy loss for >22 keV electrons due to each process.

A. TOTAL ENERGY LOST THROUGH ESCAPING ELECTRONS

The total energy loss from escaping electrons, $\mathscr{E}_{\text{escape}}(E>E_0)$, is easily calculated,

$$\mathscr{E}_{\text{escape}}(E > E_0) = N_{\text{escape}}(E > E_0)\,\bar{E} \tag{12}$$

where $\bar{E}$ is the average electron energy. We assume here that no appreciable coronal trapping occurs.

* We have not imposed a cutoff at 100 keV in calculating the spectral exponent of the escaping electrons. A cutoff at 100 keV would decrease values of $|\delta|$ by ~0.4.

B. TOTAL ENERGY LOST BY COLLISIONS

For electrons of a given energy the energy loss due to collisions is directly proportional to the bremsstrahlung energy loss. We compute the ratio of bremsstrahlung energy loss to collision energy loss for both fully ionized hydrogen and neutral hydrogen. From Trubnikov (1965) and Takakura (1969), we obtain for fully ionized hydrogen and $E \lesssim 100$ keV,

$$-\left(\frac{dE}{dt}\right)_{\substack{\text{collision}\\ \text{ionized}}} = 4.9 \times 10^{-9}\, n_i E^{-1/2} \text{ keV/sec} \tag{13}$$

where E is in keV and n_i is cm^{-3}. Bremsstrahlung energy loss is given by Berger and Seltzer (1964) over the energy range 10–100 keV and can be closely approximated by

$$-\left(\frac{dE}{dt}\right)_{\text{brems}} = 6.2 \times 10^{-18}\, n_i E^{1/2}(E + 988) \text{ keV/sec}. \tag{14}$$

The ratio of the bremsstrahlung loss rate to the collision loss rate in an ionized medium is dependent only on the energy of the electron since the ion density n_i cancels out. This ratio is averaged over the assumed power law electron spectrum (Equation 1) in the energy range 22–100 keV,

$$\bar{R}(\delta) = \frac{\int_{22}^{100} \left(\frac{dE}{dt}_{\text{brems}}\right)\left(\frac{dE}{dt}_{\text{collision}}\right)^{-1} \frac{dn_e}{dE}\, dE}{\int_{22}^{100} \frac{dn_e}{dE}\, dE}, \tag{15}$$

to obtain the values of $\bar{R}(\delta)_{\text{ionized}}$ plotted in Figure 6. For neutral hydrogen we obtain from Evans (1955),

$$-\left(\frac{dE}{dt}\right)_{\substack{\text{collision}\\ \text{neutral}}} = \frac{2\pi e^4}{m_0 C}\frac{n_i}{\beta}\left\{\ln\left[\frac{2E^2}{I^2(1-\beta^2)}\right] - \beta^2\right\} \text{ ergs/sec} =$$

$$= 7.76 \times 10^{-12}\frac{n_i}{\beta_i}\left\{\ln\left[\frac{2E^2}{1.85 \times 10^{-4}(1-\beta^2)}\right] - \beta^2\right\} \text{ keV/sec} \tag{16}$$

where $\beta = v/c$. $\bar{R}(\delta)_{\text{neutral}}$ is calculated numerically and also graphed in Figure 5. The ionized and neutral medium values differ roughly by a factor of 2 and both ratios are $\sim 10^{-4}$ compared to $\sim 10^{-3}$ for relativistic electrons. Furthermore, note that in both energy loss equations (ionized and neutral) the rate of energy loss *increases* for decreasing energy.

Using $\bar{R}(\delta)$ the total collision energy loss is computed as follows: First, δ is ob-

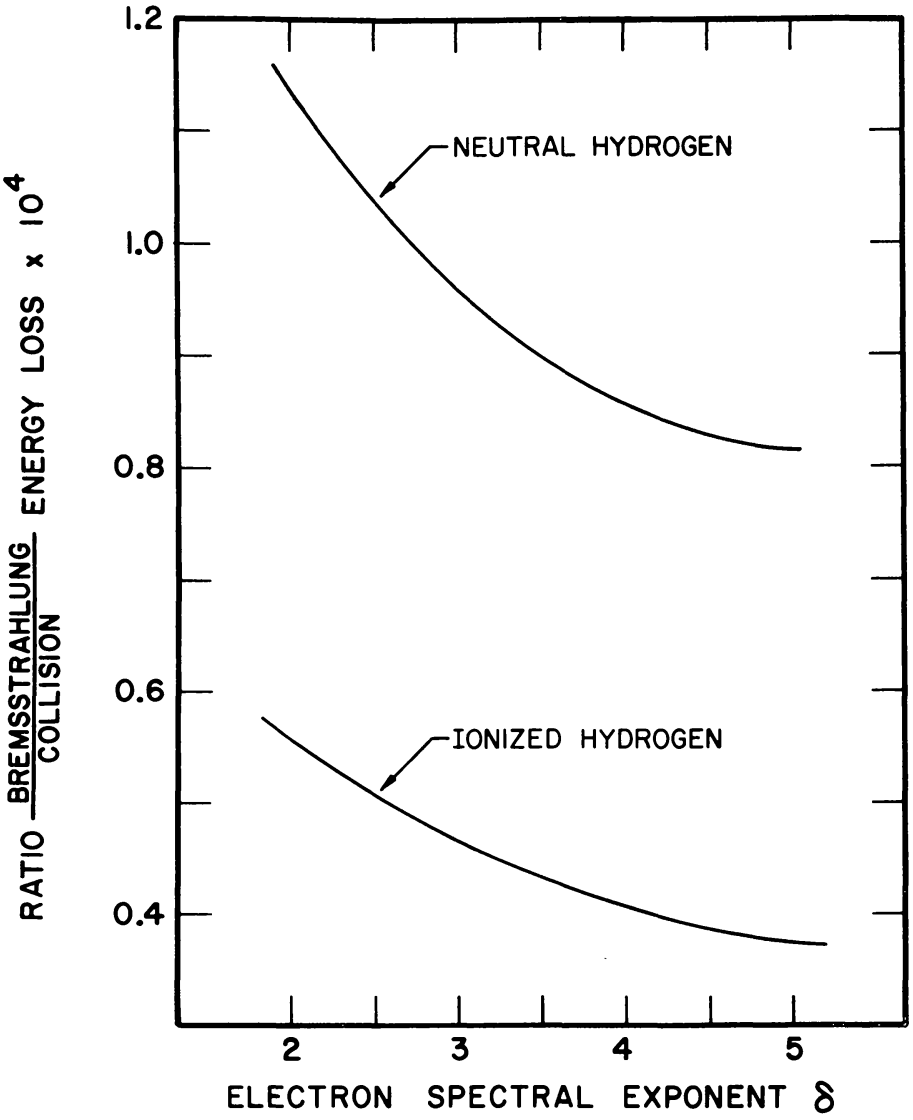

Fig. 6. The ratio of electron energy loss by bremsstrahlung to energy loss by collisions for both neutral and ionized hydrogen is shown here as a function of the electron spectral exponent. The energy losses are averaged over the electron spectrum in the energy range 22–100 keV.

tained as outlined previously (Section 3). Then integrating $\mathrm{d}J(h\nu)/\mathrm{d}(h\nu)$ over the time of the non-thermal X-ray burst and over energy, we obtain the total energy lost by bremsstrahlung

$$\mathscr{E}_{\text{brems}}(h\nu > 22) = 4\pi r^2 \int_{22}^{100} \left(\int_{\text{spike}} h\nu \frac{\mathrm{d}J(h\nu, t)}{\mathrm{d}(h\nu)} \mathrm{d}t \right) \mathrm{d}(h\nu). \tag{17}$$

Adding on the bremsstrahlung energy loss from photons below 22 keV due to above 22 keV electrons, we obtain

$$\mathscr{E}_{\text{brems}}(h\nu > 0) = 4\pi r^2 G(\delta) \int_{\text{spike}} J(22\ \text{keV} < h\nu < 38\ \text{keV})\, \mathrm{d}t \tag{18}$$

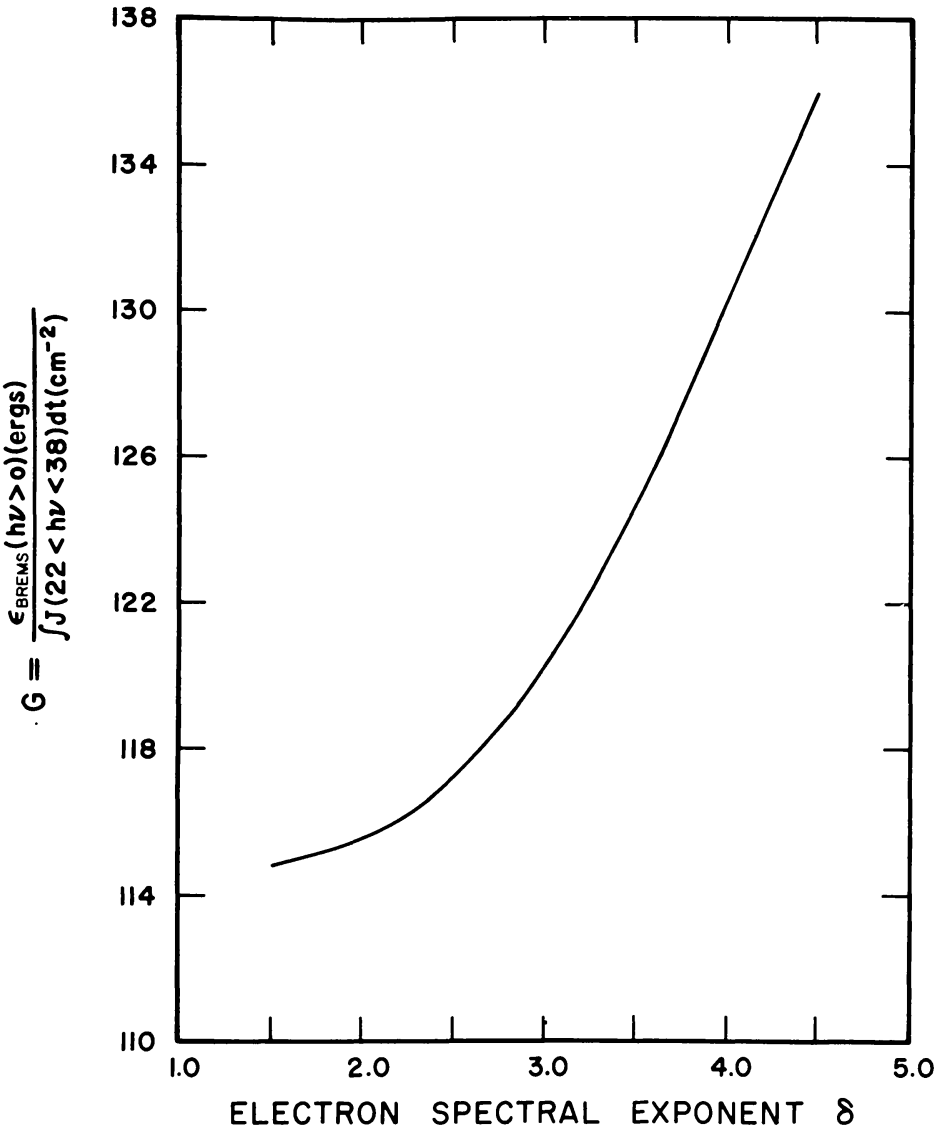

Fig. 7. This factor G relates the integrated photon flux for 22 keV $< h\nu <$ 100 keV to the total bremsstrahlung energy loss for electrons of energy 22–100 keV. G is graphed as a function of the electron spectral exponent δ.

where the parameter $G(\delta)$ is graphed in Figure 7. Then, the total energy lost by collision is

$$\mathscr{E}_{\text{collision}}(E > 22 \text{ keV}) = \bar{R}(\delta)\, \mathscr{E}_{\text{brems}}(h\nu > 0). \tag{19}$$

$\mathscr{E}_{\text{brems}}(h\nu > 0)$, $\mathscr{E}_{\substack{\text{collision} \\ \text{neutral}}}(E > 22 \text{ keV})$ and $\mathscr{E}_{\substack{\text{collision} \\ \text{ionized}}}(E > 22 \text{ keV})$ have been calculated and tabulated in Table II for each of the five events studied.

The computed collision energy losses are lower limits to the actual energy losses since they do not take into account collective plasma effects (Friedman and Hamberger, 1969). These effects are such as to increase the electron energy losses without affecting the bremsstrahlung X-ray production.

TABLE II

Total numbers and energies of non-thermal electrons in various solar processes [a]

Date 1967	X-ray maximum UT	Optical flare		Energy losses (erg)				Total electron energy ε_{total} (ergs)	Number of electrons			
		Importance	Location	ε_{brems}	$\varepsilon_{collision}$		ε_{escape}		Total [b] accelerated	At X-ray [c] maximum	Total escaped	Producing [d] microwave emission
					Ionized	Neutral						
30 July	0509.1	1*B*	N25 W29	2.9×10^{24}	7.4×10^{28}	3.4×10^{28}	2.1×10^{26}	9.9×10^{28}	5.1×10^{36}	3.3×10^{35}	2.9×10^{33}	5.0×10^{29}
30 July	1601.0	– *B*	N13 W07	9.7×10^{23}	2.2×10^{28}	1.1×10^{28}	1.8×10^{26}	6.4×10^{28}	1.2×10^{36}	2.2×10^{35}	2.6×10^{33}	5.5×10^{29}
3 August	0921.7	1*B*	N27 W85	3.4×10^{24}	8.2×10^{28}	3.9×10^{28}	4.4×10^{26}	1.0×10^{29}	5.1×10^{36}	5.8×10^{35}	6.7×10^{33}	1.1×10^{30}
25 October	2129.7	– *B*	N10 W35	3.2×10^{23}	7.7×10^{27}	3.7×10^{27}	3.2×10^{25}	9.6×10^{27}	4.8×10^{35}	7.8×10^{34}	5.5×10^{32}	–
13 December	1436.0	– *F*	N15 W71	1.1×10^{24}	2.5×10^{28}	1.2×10^{28}	4.4×10^{25}	3.3×10^{28}	1.6×10^{36}	1.3×10^{35}	6.3×10^{32}	3.6×10^{29}

[a] All numbers (energies and number of electrons) calculated for $E > 22$ keV electrons.
[b] Calculated with the $\varepsilon_{collision}$ in ionized medium.
[c] Calculated assuming density $n_i = 3.5 \times 10^{10}$.
[d] Number of electrons between 22 and 500 keV.

Finally, we note that this method of computation of collisional energy losses from bremsstrahlung energy losses is *not* dependent on the ambient density nor is it dependent on the electron stopping in the gas (as in thick target theory).

It is apparent from Table II that for the events studied (keeping in mind the instrumental limitations by which these events were chosen for analysis) the energy loss due to collisions with the ambient medium completely dominates over energy loss due to electrons escaping into the interplanetary medium. A possibility which cannot be ruled out at the present time is that a large fraction of the electrons escape into the corona, there to be trapped. If we assume that coronal trapping does not take place, we may attribute the decay of the X-ray bursts to collision processes since the only other energy loss mechanism, synchrotron radiation, leads to a decay time constant of $\gtrsim 10^2$ sec for 10–100 keV electrons in a magnetic field of $\lesssim 10^3$ G (Snijders, 1968). Typical decay time constants for the non-thermal component of an X-ray burst are 1–10 sec (see Figure 1 and Kane and Anderson, 1970). This decay time constant is an upper limit to the time constant for electron loss processes. It is possible to have shorter time constants for loss processes if the acceleration is not instantaneous. Then the time profile of the burst would essentially reflect the time profile of the acceleration. Some evidence that this may be the case is provided by Kane and Anderson (1970) whose observations show that the higher energy channels decay more rapidly than lower energy channels for the non-thermal X-ray component, just the reverse of the expected energy dependence for collisional energy loss. They interpret these observations to imply that a combination of escape and collision processes dominate the decay phase of the burst, but our analysis here indicates that escape processes, at least escape into the interplanetary medium, do not play a significant role in determining the decay of the X-ray burst.

For purposes of constructing a consistent picture of the electron acceleration event we shall assume that the *e*-folding time constant for energy loss due to collisions is on the order of 1 sec. For our calculations we shall assume a completely ionized medium although the results would be essentially unchanged for a neutral medium. From Equation (13) we obtain

$$\tau_c \approx \frac{10^8}{n_i} E^{3/2} \tag{20}$$

as the time for an electron to lose $1-1/e$ of its initial energy (E in keV). For $E \sim 50$ keV, we obtain $n_i \sim 3.5 \times 10^{10}$ cm^{-3}.

For our calculated values of $n_e n_i V$ at non-thermal X-ray burst maximum (Table I) we obtain $N_{\max}(E > 22 \text{ keV}, t)$ for $n_i = 3.5 \times 10^{10}$. This number is tabulated in Table II for each event.

6. Acceleration of Finite Duration

If the acceleration is essentially instantaneous compared to electron loss times then indeed the number of electrons producing the X-rays at burst maximum will be just the total number of electrons produced. However, if the acceleration extends over a

time scale long compared to the time scale of the particle loss mechanisms then the total number of electrons produced will be greater than the number in the source region at any instant of time, i.e., the number inferred from X-ray burst maximum. To see whether the picture of extended electron acceleration is consistent we compare $N_{\max}(E>22\text{ keV}, t)$ with the total number accelerated, $N_{\text{total}}(E>22\text{ keV})=\mathscr{E}_{\text{total}}(E>22\text{ keV})/\bar{E}$, where $\mathscr{E}_{\text{total}}(E>22\text{ keV})$ is the total energy in electrons accelerated above 22 keV and $\bar{E}$ is the average electron energy. Neglecting $\mathscr{E}_{\text{escape}}(E>22\text{ keV})$, we have

$$\mathscr{E}_{\text{total}}(E>22\text{ keV}) = \mathscr{E}_{\text{collision}}(E>22\text{ keV}) + \\ + N_{\text{total}}(E>22\text{ keV}) \times 22\text{ keV} \times 1.6\times 10^{-9}\,(\text{erg/keV})$$

or substituting $N_{\text{total}}\bar{E}$ for $\mathscr{E}_{\text{total}}$

$$N_{\text{total}}(E>22\text{ keV}) = \frac{\mathscr{E}_{\text{collision}}(E>22\text{ keV})}{1.6\times 10^{-9}(\bar{E}-22)}$$

and

$$\mathscr{E}_{\text{total}}(E>22\text{ keV}) = \frac{\bar{E}}{\bar{E}-22}\,\mathscr{E}_{\text{collision}}(E>22\text{ keV}). \tag{21}$$

These quantities are listed in Table II for each event. For $n_i\approx 3.5\times 10^{10}$ cm^{-3}, corresponding to $\tau_c\approx 1$ sec, $N_{\text{total}}(E>22\text{ keV})$ is about ten times $N_{\max}(E>22\text{ keV}, t)$. Of course, had we assumed $\tau_c\approx 10$ sec, then $N_{\text{total}}(E>22\text{ keV})\approx N_{\max}(E>22\text{ keV}, t)$. Similarly, for smaller values of τ_c, correspondingly larger ratios of N_{total} to $N_{\max}$ would be obtained. Thus, the observations presented here cannot by themselves rule out either instantaneous acceleration with $\tau_c\sim 10$ sec, or $\tau_c<1$ sec (which would correspond to higher densities). In this respect it is useful to note that a close correlation exists between non-thermal X-ray bursts and EUV bursts (Kane and Donnelly, 1971). EUV emission is produced in the solar atmosphere at densities of $\sim 10^{11-12}$ cm^{-3}.

Using the assumed values of $\tau_c\approx 1$ sec we can derive a number for the duration of the acceleration. Suppose the acceleration of electrons proceeds over a time τ_a; for convenience sake we will assume that the acceleration is constant over that time. We may write the following equation for the particle population in the acceleration region:

$$\frac{\partial N(E,t)}{\partial t} = f(t) - \frac{N(E,t)}{\tau_e} + \frac{\partial}{\partial E}\left(N(E,t)\frac{\mathrm{d}E}{\mathrm{d}t}\right) \tag{22}$$

where N is the number of particles, $f(t)$ is the acceleration function and τ_e is the escape time constant. The second term on the right is due to particles escaping from the region. The third term on the right is the energy loss (or gain) term. In this context this term is due to collisional energy losses. We will simplify our calculations by replacing the third term with $-[N(E,t)/\tau_c]$. Finally we take

$$f(t)=A \qquad 0<t<\tau_a$$
$$f(t)=0 \qquad t<0,\ t>\tau_a$$

where τ_a is a characteristic acceleration duration. Then we obtain

$$0 < t < \tau_a \qquad \frac{\partial N}{\partial t} = A - \frac{N}{\tau_L} \quad \text{where} \quad \tau_L = \frac{\tau_e \tau_c}{\tau_e + \tau_c}$$

$$t > \tau_a \qquad \frac{\partial N}{\partial t} = -\frac{N}{\tau_L}. \tag{23}$$

Solving with boundary condition that $N=0$ at $t=0$, we obtain

$$\begin{aligned} N(t) &= A\tau_L(1 - e^{-t/\tau_c}) \qquad 0 < t < \tau_a \\ &= A\tau_L(e^{\tau_a/\tau_L} - 1)\, e^{-t/\tau_L} \qquad t > \tau_a. \end{aligned} \tag{24}$$

The total number accelerated is

$$N_{\text{total}} = A\tau_a$$

and the maximum number in the acceleration region at any instant is

$$N(t)_{\max} = A\tau_L(1 - e^{-\tau_a/\tau_L}).$$

The ratio is then

$$\frac{N_{\text{total}}}{N(t)_{\max}} = \frac{\tau_a}{\tau_L} \frac{1}{1 - e^{-\tau_a/\tau_L}}. \tag{25}$$

As we noted in the earlier discussion, for $\tau_a \ll \tau_L$, $N_{\text{total}}/N(t)_{\max} \approx 1$. However for $\tau_a \gg \tau_L$, we obtain

$$\frac{N_{\text{total}}}{N(t)_{\max}} \approx \frac{\tau_a}{\tau_L}. \tag{26}$$

This last equation implies that the number of electrons, $N_{\max}(t)$, derived from the maximum X-ray flux is smaller by a factor τ_a/τ_L than the total number accelerated.

For our case where $N_{\text{total}}/N(t)_{\max} \approx 10$ and $\tau_L \approx \tau_c \approx 1$ sec, we have $\tau_a \approx 10$ sec. This agrees well with the observed durations of the non-thermal component of X-ray bursts, particularly in view of the numerous assumptions made here.

To explain the observed inverse relationship between the rise and decay times of the non-thermal component and the X-ray energy, the acceleration process must not only be extended in time but the average energy of the accelerated electrons must first increase and then decrease through the event. This variation is not unreasonable to expect from acceleration processes.

Another argument for extended acceleration is that instantaneous acceleration would imply a characteristic shape for the intensity-time profile of the non-thermal X-ray burst, namely, essentially an exponential (e^{-t/τ_L}) decay after the initial spike. Many non-thermal bursts have been observed with differing shapes.

7. Discussion

A. ELECTRON ACCELERATION IN SOLAR FLARES

For the very large optical importance 3+ flares which produce energetic protons as well as electrons the total energy content in non-thermal particles is on the order of a few times 10^{31} erg (Bruzek, 1967) compared to a total optical emission of $\sim 10^{32}$ erg and a total flare energy, including the interplanetary blast wave, of $\sim 2 \times 10^{32}$ erg. A rather similar energy balance exists for these small flares and subflares which have been analyzed here. Table II lists the optical importance of each flare event. Smith and Smith (1963) give values of $\sim 10^{29}$ erg for the Hα emission from an importance 2 flare. Hudson *et al.* (1969) estimate $\sim 10^{29}$ erg for the quasi-thermal energy in these small importance 1 flare or subflares based on a temperature-emission measure analysis of the quasi-thermal component of the X-ray burst. Kahler *et al.* (1970) in a similar analysis utilizing proportional counter data obtain similar numbers. This compares to $\sim 5 \times 10^{28}$ erg in >22 keV electrons and more if the spectrum is extended to lower energies. However, as we have pointed out, the event selection process is such that only the relatively intense non-thermal bursts are chosen for analysis. For many other flares from which escaping electrons are observed but not an intense non-thermal X-ray component, the energy content in these particles may be much less. An alternative possibility is that the energy content in accelerated electrons is still of the same order but that the height of production of the energetic electrons may vary from flare to flare. In some flares, such as the ones analyzed, the electron production occurs low in the solar atmosphere and thus generates intense non-thermal X-ray emission. In other flares the electrons are accelerated high up in corona where the ion density is low and therefore the X-ray emission is small. Those types of events would provide escaping electrons without substantial non-thermal X-ray emission.

For the events analyzed the acceleration of electrons to 10–100 keV energies must be a highly efficient process to account for the roughly comparable energies in the quasi-thermal/optical flare and in energetic electrons. It is energetically possible for the non-thermal electrons to heat the flare region to produce the optical and quasi-thermal flare as proposed by Kahler *et al.* (1970). However, such an interpretation fails for the events in which no non-thermal radiation is observed above the background of the detector.

In the events analyzed we can place stringent requirements on the electron acceleration mechanism in the flare:

(1) It must be highly efficient; roughly equal amounts of energy must go into non-thermal particles and into the quasi-thermal flare.

(2) It must accelerate the particles on a time scale of ~ 10 sec.

(3) The accelerated electron energy varies through the event, going from low to high and back to low.

(4) It must be able to accelerate and emit 10–100 keV electrons without simultaneously accelerating and emitting protons to >300 keV energies since many electron events are observed without protons above 300 keV. That is to say, equal particle

velocity acceleration mechanisms are ruled out. Of these restrictions, clearly the first one is the most difficult to meet. Basically the flare mechanism must be such as to accelerate large numbers of particles as a primary energy dissipation process. To our knowledge two flare mechanisms, those of Alfvén and Carlqvist (1967) and Syrovatsky (1969) have been proposed which meet this requirement. Both these mechanisms depend on the increase of the current density carried by a plasma beyond its stable current limit, leading to large electric fields. In Alfvén and Carlqvist's model, steady currents following magnetic field lines in the solar atmosphere generate very high current densities when local constrictions of the magnetic field (due to pinch effect or similar phenomena) occur. This current interprution produces a large inductive electric field which results in the release of most of the magnetic energy in the circuit at the point of the interruption. A large part of the energy goes into accelerating particles. Total magnetic energy released will be on the order of 0.5×10^{30} erg and particles may be accelerated up to 10^9 eV.

Syrovatsky considers the flow of plasma toward a magnetic neutral sheet. The currents which must flow along the thin neutral sheet may lead to large current densities that exceed the stable current density for a plasma. For typical conditions in a solar flare region, the resulting electric field accelerates particles along the sheet as the main form of energy dissipation. Total energy available is $\sim 10^{28}$ to 10^{32} erg and particles can be accelerated to a maximum rigidity of 10^{11} to 10^{15} V. Of course, for the events studied here these mechanisms may be scaled down somewhat from their maximum values. One possible way of distinguishing between these two alternatives is through observation of 10–100 keV solar cosmic ray protons. Alfvén and Carlqvist's model leads to electrons and protons of the same energy while Syrovatsky's model leads to particles of the same rigidity.

B. ELECTRON LOSS BY ESCAPE

Having examined the electron acceleration process, we now turn to the escape process. First the efficiency of escape is small for these events: $N_{\text{escape}}/N_{\text{total}} \approx 10^{-3}$ so the efficiency is on the order of 0.1%. This result is similar to that derived by Cline and McDonald (1968) for relativistic electrons in the 7 July 1966 event. However, it must be pointed out here that these events are selected ones in which the non-thermal X-ray burst is intense. For many events (for example, those 8 in which no non-thermal component was observed), a much higher escape efficiency must prevail.

A comparison of the energy spectra of the escaping electrons versus the X-ray producing ones clearly shows that the escaping electrons are more energetic. This effect is qualitatively consistent with the energy dependence of the mean free path of charged particles in the solar atmosphere. The argument has been presented by De Jager (1960) and goes as follows: The mean free path for charged particles with velocity $\sim 10^5$ km/sec (~ 30 keV) is approximately equal to the scale height of the corona ($\sim 5 \times 10^4$ km) and decreases rapidly with decreasing velocity. Thus low energy ($\lesssim 30$ keV) electrons are likely to be stopped in the solar atmosphere while high energy electrons will escape.

C. RADIO EMISSION

We have examined the maximum flux observed in the accompanying microwave radio burst at $\sim 10^4$ Hz for each event (*IAU Quartely Bulletin on Solar Activity*). Using the scaling factor given by Takakura (1968) for fields of $\sim 10^3$ G and electron spectral exponent $\delta \approx 3$ (~ 100 flux units $\Rightarrow 10^{29}$ electrons in 50–500 keV range) we have converted these microwave fluxes into number of electrons in the energy range 50–500 keV. Then using the spectral exponents derived from the X-ray emission, we have computed the radio-emitting population of electrons above 22 keV. These numbers are given in Table II and are typically $\sim 10^{29}$–10^{30} electrons. Note that the ratio of radio-emitting electrons to X-ray producing electrons (at burst maximum) is essentially constant, $(N_R/N_X) \sim 5 \times 10^5$. The one X-ray event for which a radio event was not reported is also the smallest.

We have also looked for type III emission accompanying these events. For the first two events relatively intense type III burst are observed coincident with the X-ray maximum. No radio data was available for the 3 August event, and no type III emission was observed for the last two events. The first two events released ~ 5 times as many electrons as the last two events.

8. Conclusions

We have analyzed the emission of 10–100 keV X-rays and electrons from five small solar flares. We find that:

(1) The electron energy spectra, assuming a power law form in the range 22–100 keV, have exponents of ~ 3.5–4.2 for the X-ray producing electrons and ~ 2.91–3.17 for the escaping electrons. The emission measure, $n_e(E > 22 \text{ keV}) n_i V$, at maximum varied from $\sim 2.7 \times 10^{45}$ to 1.15×10^{46} cm^{-3} and the total number of escaping electrons with energy > 22 keV varied from $\sim 5 \times 10^{32}$ to 6.7×10^{33}.

(2) The total energy loss due to collisions in the solar atmosphere was calculated from the total bremsstrahlung energy loss. For > 22 keV electrons typical values for the total energy in various processes are:

$$\mathscr{E}_{\text{brems}} \sim 3 \times 10^{23} - 3 \times 10^{24} \text{ erg}$$

$$\mathscr{E}_{\substack{\text{collision} \\ \text{ionized}}} \sim 7 \times 10^{27} - 8 \times 10^{28} \text{ erg}, \left(\mathscr{E}_{\substack{\text{collision} \\ \text{neutral}}} \sim \tfrac{1}{2} \mathscr{E}_{\substack{\text{collision} \\ \text{ionized}}}\right)$$

$$\mathscr{E}_{\text{escape}} \sim 3 \times 10^{25} - 4 \times 10^{26} \text{ erg}$$

$$\mathscr{E}_{\text{total}} \sim 10^{28} - 10^{29} \text{ erg}$$

Total number of electrons accelerated above 22 keV is $\sim 10^{36}$.

(3) A consistent picture of electron acceleration, energy loss and escape during these flares was developed. This picture consisted of:

(a) electron acceleration over the ~ 10–100 sec duration of the non-thermal X-ray emission, with the average energy of the accelerated particles increasing and then decreasing through the burst;

(b) electron energy loss predominantly by collisions on a short time scale, ~ 1 sec, compared with the acceleration. This time scale leads to an ambient ion density $n_i \approx 3 \times 10^{10}$ cm^{-3};

(c) escape of electrons into the interplanetary medium with efficiency of ~ 0.1–1% and predominantly of the higher energy electrons;

(d) total numbers of >22 keV electrons of $\sim 5 \times 10^{35}$–5×10^{36} and total energy in electrons of $\sim 10^{28}$–10^{29} erg as compared to $\sim 10^{29}$ erg in the quasi-thermal flare.

(4) A large fraction ($\sim \frac{1}{2}$) of the total flare energy is contained in non-thermal electrons, implying that the electron acceleration must be a major energy dissipation mechanism for the flare mechanism. The flare mechanisms of Alfvén and Carlqvist and Syrovatsky are discussed.

Acknowledgements

We wish to acknowledge extensive discussions with Dr. S. R. Kane. Professor K. A. Anderson, Professor L. E. Peterson and Mr. D. MacKenzie provided valuable asistance in many phases of this work.

This work was supported in part by the National Aeronautics and Space Administration under grant NGL-05-003-017 and contract NAS 5-9091 at the University of California, Berkeley and contract NAS 5-3177 at the University of California, San Diego.

References

Alfvén, H. and Carlqvist, P.: 1967, *Solar Phys.* **1**, 220.
Anderson, K. A. and Winckler, J. R.: 1962, *J. Geophys. Res.* **67**, 4103.
Arnoldy, R. L., Kane, S. R., and Winckler, J. R.: 1968, *Astrophys. J.* **151**, 711.
Berger, M. J. and Seltzer, S. M.: 1964, 'Tables of Energy Losses and Ranges of Electrons and Positrons', NASA SP-3012.
Bruzek, A.: 1967, 'Physics of Solar Flares: The Energy and Mass Problem', in *Solar Physics* (ed. by John Xanthakis), Interscience Publishers, p. 399.
Cline, T. L. and McDonald, F. B.: 1968, *Solar Phys.* **5**, 507.
De Jager, C.: 1955, *Ann. Geophys.* **11**, 330.
Evans, R. D.: 1955, *The Atomic Nucleus*, p. 582.
Friedman, M. and Hamberger, S. M.: 1969, *Solar Phys.* **8**, 104.
Holt, S. S. and Cline, T. L.: 1968, *Astrophys. J.* **154**, 1027.
Hudson, H. S., Peterson, L. E., and Schwartz, D. A.: 1969, *Astrophys. J.* **157**, 389.
Jackson, J. D.: 1962, *Classical Electrodynamics*, Ch. 15, John Wiley & Sons, New York.
Kahler, S. W., Meekins, J. F., Kreplin R. W., and Bowyer, C. S.: 1970, 'Temperature and Emission Measure Profiles of Two Solar X-ray flares, submitted to *Astrophys. J.*
Kane, S. R. and Anderson, K. A.: 1970, *Astrophys. J.* **162**, 1003.
Kane, S. R. and Donnelly, R. F.: 1971, *Astrophys. J.* **164**, 151.
Kane, S. R. and Hudson, H. S.: 1970, *Solar Phys.* **14**, 414.
Kundu, M. R.: 1965, *Solar Radio Astronomy*, Ch. 2, Interscience Publishers.
Lin, R. P.: 1970a, *Solar Phys.* **12**, 266.
Lin, R. P.: 1970b, *Solar Phys.* **15**, 453.
Lin, R. P.: 1970c, *J. Geophys. Res.* **75**, 2583.
Lin, R. P. and Anderson, K. A.: 1967, *Solar Phys.* **4**, 338.
Lin, R. P. and Anderson, K. A.: 1970, 'Energy Spectra of Solar Flare Electrons' (in preparation).
Parker, E. N.: 1963, *Interplanetary Dynamical Processes*, Ch. 8, Interscience Publishers.
Smith, H. J. and Smith, E. P.: 1963, *Solar Flares*, Macmillan Co., New York.

Snijders, R.: 1968, *Solar Phys.* **4**, 432.
Syrovatsky, S. I.: 1969, 'On the Mechanism of Solar Flares', in *Solar Flares and Space Research* (ed. by C. de Jager and Z. Švestka), North-Holland Publ. Co., Amsterdam, p. 346.
Takakura, T.: 1969, *Solar Phys.* **6**, 133.
Trubnikov, B. A.: 1965, *Rev. Plasma Phys.* **1**, 105.